J. Mol. Model. **1998**, *4*, 221 – 233

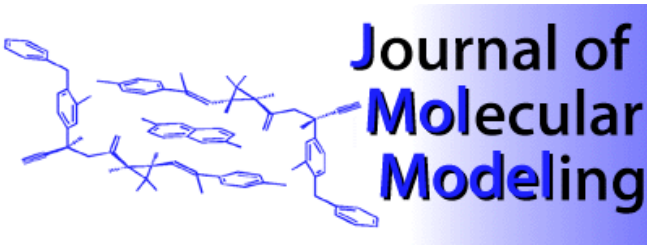

FULL PAPER

Molecular Modeling of the NPY Binding Site on the Y_1 Receptor

Ingebrigt Sylte[1], Catherine Robin-Jagerschmidt[2,†], Claire Bihoreau[2], Luce Hendricksen[2], Alain Calvet[2], Claude Bénicourt[2,‡], and Svein G. Dahl[1]

[1]Department of Pharmacology, Faculty of Medicine, University of Tromsø, N-9037 Tromsø, Norway. Tel: +4777644875; Fax: +4777645310. E-mail: sylte@fagmed.uit.no

[2]Institut de Recherche Jouveinal, 3-9, rue de la Loge, 94265 Fresnes Cedex, France

Received: 19 March 1998 / Accepted: 2 July 1998 / Published: 10 July 1998

Abstract A three-dimensional model of the neuropeptide Y (NPY) - rat Y_1 (rY_1) receptor complex and of the NPY_{13-36} - rY_1 receptor complex was constructed by molecular modeling based on the electron density projection map of rhodopsin and on site-directed mutagenesis studies of neuropeptide receptors. In order to further guide the modeling, the nucleotide sequences encoding Trp287, Cys295 and His297 in the third extracellular loop of the rY_1 receptor, were altered by site-directed mutagenesis experiments. Single-point mutated receptors were expressed in COS-7 cells, and tested for their ability to bind radio labelled NPY (^{3}H-NPY). Mutations of Trp287 and His297 completely abolished binding of ^{3}H-NPY. The Cys295Ser mutation only slightly decreased the binding of ^{3}H-NPY, suggesting that the involvement of Cys295 in a disulphide bond is not essential for maintaining the correct three-dimensional structure of the binding site for NPY. Molecular dynamics simulations of NPY-rY_1 receptor interactions suggested that Asp199, Asp103 and Asp286 in the receptor interact, respectively, with Lys4, Arg33 and Arg35 of NPY. The simulations also suggested that His297 acts as a hydrogen acceptor from Arg35 in NPY, and that Tyr1 of NPY interacts with a binding pocket on the receptor formed by Asn115, Asp286, Trp287 and His297. Tyr36 in NPY interacted both with Thr41 and Tyr99 via hydrogen bonds, and also with Asn296, His297 and Phe301. The present study suggests that amino acid residues at the extracellular end of the transmembrane helices and in the extracellular loops are strongly involved in binding to NPY and NPY_{13-36}.

Keywords NPY, rY_1 receptor, Site-directed mutagenesis, Binding site, Molecular dynamics

Introduction

Neuropeptide Y (NPY) belongs to the PP family of structurally related peptides, which also includes gut peptide YY (PYY) and pancreatic polypeptide (PP). All these peptides have a primary structure of 36 amino acids and an amidated C-terminal end. It has been suggested that they feature a three-dimensional structure consisting of an N-terminal

Correspondence to: I. Sylte
[†]*Present address:* Hoechst Marion Roussel, 102 route de Noisy, F-93235 Romainville Cedex, France.
[‡]*Present address:* Ecole Normale Supérieure de Cachan, 61, avenue du Président Wilson, F-94235 Cachan Cedex, France.

polyproline helix (residue 1-8), an amphipatic α-helix (residue 15-30), and a β-turn creating a hairpin-like loop [1-3].

Receptor binding studies using NPY, PYY, PP and NPY analogs have identified six receptor subtypes distinguished by their affinity for the PP-family of peptides:

- Y_1: PYY ≥ NPY ≥ [Leu31, Pro34]NPY >> NPY_{13-36} > PP [4, 5],
- Y_2: PYY ≥ NPY > NPY_{13-36} >> [Leu31, Pro34]NPY [6],
- Y_3: NPY > [Pro34]NPY > NPY_{13-36} > PP >> PYY [7],
- Y_4: PP > PYY > NPY ≥ [Leu31, Pro34]NPY > NPY_{2-36} ≥ NPY_{13-36} [8, 9],
- Y_5: NPY = PYY = [Leu31, Pro34]NPY = NPY_{2-36} > NPY_{13-36} > PP [10, 11],
- PYY preferring receptor: PYY > NPY > [Leu31, Pro34]NPY > PP > NPY_{2-36} >> NPY_{13-36} [12].

The Y_1 receptor, which is presently the best characterized NPY receptor subtype, is generally considered to be postsynaptic, and to mediate many of the peripheral actions of NPY including most of its cardiovascular effects, and potential anxiolytic effects. The Y_1 receptor therefore represents an interesting molecular target for drug discovery.

Cloning and sequencing of the human Y_1 receptor (hY_1) [4, 5] and the rat Y_1 receptor (rY_1) [13, 14], have shown that the Y_1 receptor belongs to the superfamily of G protein coupled receptors (GPCR). Based on the electron density projection map of visual rhodopsin [15], and on site-directed mutagenesis studies of GPCRs, a general arrangement of the TMHs in GPCRs was proposed [16]. The general feature of this proposed arrangement were verified by the most recent projection map of frog rhodopsin [17], indicating that this arrangement may be used to construct reliable models of GPCRs by molecular modeling.

In the present study we construct a three-dimensional model of the NPY-rY_1 receptor complex based on previously reported site-directed mutagenesis studies of the hY_1 and the rY_1 receptor [18-21], and on a series of site-directed mutagenesis experiments with other neuropeptide receptors (Table 1). The majority of GPCRs contain a cysteine residue in EC1 and in EC2 which are believed to form a disulphide bridge [22]. The rY_1 receptor, and several other GPCRs also have cysteine residues in the N-terminal and in EC3, and this pair of cysteines form a disulphide bond in the angiotensin II AT_{1a} receptor [23]. Site-directed mutagenesis experiments of neuropeptide GPCRs have also shown that the third extracellular loop (EC3) is very important for binding to the neuropeptides [24]. Therefore, in order to further guide the modeling, the nucleotide sequence encoding Trp287, Cys295 and His297 in EC3 were altered by site-directed mutagenesis studies, and the mutants were tested for their ability to bind radio labelled NPY (^{3}H-NPY).

Site-directed mutagenesis experiments

Cellular and bacterial culture media were obtained from GIBCO BRL, and restriction enzymes and *Taq* DNA polymerase from Boehringer Mannheim. Cell lines were obtained from the American Type Culture Collection. Oligonucleotides were synthesized on a PCR-mate EP 391 synthesizer from Applied Biosystems. When necessary, the oligonucleotides were purified by High Performance Liquid Chromatography with a Delta park C18-300 Å (3.9 mm x 15 cm) Reverse-Phase column Waters (Millipore). PCR reactions were performed on a LEP scientific thermocycler. ^{3}H-labelled porcine NPY was purchased from Amersham (Specific activity: 65 Ci. mmol^{-1}).

Cloning of rY_1 receptor cDNA

A random-primed rat hippocampal cDNA λgt11 library (Clontech) was probed at high stringency with a 1.2 kpb ^{32}P-labelled fragment obtained with RT-PCR ("Random Primed DNA Labelling Kit", Boehringer Mannheim). RT-PCR was performed using oligonucleotides synthesized according to the nucleotide sequence of the rY_1 receptor DNA [14]. The sense (FC5-5) and the antisense (FC5-3) primers corresponded to nucleotides (67-89) and (1213-1235) of the nucleic acid sequence, respectively. The cDNA from a clone containing the entire coding region and the non coding sequences of the rY_1 receptor was purified and subcloned into pKS+ (Stratagene) and pcDNA3 (InVitrogen, San Diego), leading to pKS+/rY_1 and pcDNA3/rY_1. The cDNA of this clone was entirely sequenced using a "Quick-Denature Plasmid Sequencing Kit" (USB).

Mutagenesis

The rY_1 receptor cDNA was mutated using the "Sculptor *in vitro* Mutagenesis Systems version 3".0 (Amersham), with pKS+/rY_1 as a template for the synthesis of single-strand with the helper phage VCS-M13 (Stratagene). The sequences of the coding strands used as template for site-directed mutagenesis were as follows:

Trp287Ser; CACAAGCTG**AGC**TTAGTGGTC.
Trp287Gly; ACACAAGCTG**CCC**TTAGTGGT.
Cys295Ser; GTAACGGTGG**TCG**TTGGTGTT.
His297Asn; GTGGACGTTG**TTG**TTAGACGA.

The mutated codons are underlined, whilst the mutated bases in the codons are indicated in bold. After subcloning of the mutated cDNAs into pcDNA3, and expression in COS-7 cells, ^{3}H-NPY binding was analyzed. The mutants that did not show any affinity for ^{3}H-NPY were entirely sequenced.

Binding assays on whole cells

COS-7 cells were transiently transfected with the wild type or mutated cDNAs cloned into pcDNA3 using the DEAE Dextran method. Seeded cells were treated with serum-free medium containing DEAE-Dextran (1mg·ml^{-1}) and DNA (10 μg) for 90 minutes at 37°C. The medium was then replaced by serum-free medium containing chloroquine (10^{-4} M) for additional 3 hours at 37°C. Cells were then shocked with 10

Table 1 *Site-directed mutagenesis studies of neuropeptide receptors, identified from the GRAP database [24], which were used in the packing of TMHs in the rY_1 receptor model*

TMH	Receptor subtype	Reference	Corresponding amino acid in the rY_1 receptor
2	Angiontensin II AT_{1a}	[51]	Asp85
	Gonadotropin releasing hormone	[49]	Asp85
	δ-opioid	[52]	Asp85
	μ-opioid	[53]	Asp85
	Thyrotropine releasing factor	[54]	Asp85
	Gonadotropin releasing hormone	[55]	Cys92
	Neurokinin NK1	[56]	Cys92
	Neurokinin NK1	[57]	Thr96
3	Neurokinin NK1	[38]	Asn115
	Neurokinin NK2	[58]	Asn115
	μ-opioid	[53]	Gln119
	Endothelin ET_B	[59]	Cys120
	Thyrotropin releasing factor	[60]	Cys120
4	Neurokinin NK1	[38]	Phe172
	Bradykinin B2	[61]	Tyr175
5	Neurokinin NK2	[58]	Thr211
	Angiotensin AT_{1a}	[22]	Leu215
	Bradykinin B2	[61]	Leu215
	Neurokinin NK1	[56]	Leu215
	Neurokinin NK2	[58]	Leu215
6	Bradykinin B2	[61]	Leu278, Thr279, Phe285
	μ-opioid	[54]	Thr279
	Melanocortin MC1	[62]	Phe281
	Bradykinin B2	[63]	Asn282, Asp286
	Bradykinin B2	[40]	Phe285
	Angiotensin AT_{1a}	[39]	Phe285, Asp286
	Neurokinin NK1	[64]	Phe285, Asp286
7	Neurokinin NK2	[58]	Cys304
	Angiotensin AT_{1a}	[65]	Met309
	Angiotensin AT_{1a}	[66]	Thr312
	Gonadotropin releasing hormone	[49]	Asn315

% DMSO in PBS for 2 minutes. After transfection, cells were seeded at a density of $2x10^4$ cells per well, in 24-wells plates and maintained under 5% CO_2 in Dulbecco's modified Eagle's medium (DMEM) containing 10% fetal calf serum, 1mM sodium pyruvate, 20 mM HEPES and 50 $\mu g.ml^{-1}$ gentamycine.

After 48 to 72 hours of transfection, cells were incubated with increasing concentrations of ^{3}H-NPY (from 2.10^{-11}M to 10^{-8}M) in 150 mM NaCl / 5 mM KCl / 2.5 mM $CaCl_2$ / 1.2 mM KH_2PO_4 / 2.5 mM $MgSO_4$ / 10 mM HEPES / 1% BSA at pH 7.5. Non specific binding was determined by addition of unlabelled NPY at 1μM. After 90 minutes of incubation at 37°C with gentle shaking, the incubation medium was removed, cells were lysed with 0.1 M NaOH, neutralized, and the radioactivity was determined by liquid scintillation. All binding assays were performed in duplicate. The results were analysed with the EBDA/LIGAND program [25].

Molecular modeling

Molecular mechanical energy minimizations and molecular dynamics simulations were performed with the AMBER united atom force field of the AMBER 4.0 programs [26]. A distance-dependent dielectric function ($\varepsilon = r_{ij}$, r: interatomic distance) was used for calculations of electrostatic interactions. The 1-4 vdw interactions were divided by 8.0, while the 1-4 electrostatic interactions were divided by 2.0 during the calculations. Explicit water molecules were not included in the calculations. Energy minimization of the rY_1 receptor model and of NPY-receptor interactions was done by 500 cycles of steepest descent minimization followed by 2000 cycles of conjugate gradient minimization. Molecular dynamics simulations were performed at 310 K, with velocity scaling, after an initial equilibrium period. The SHAKE option

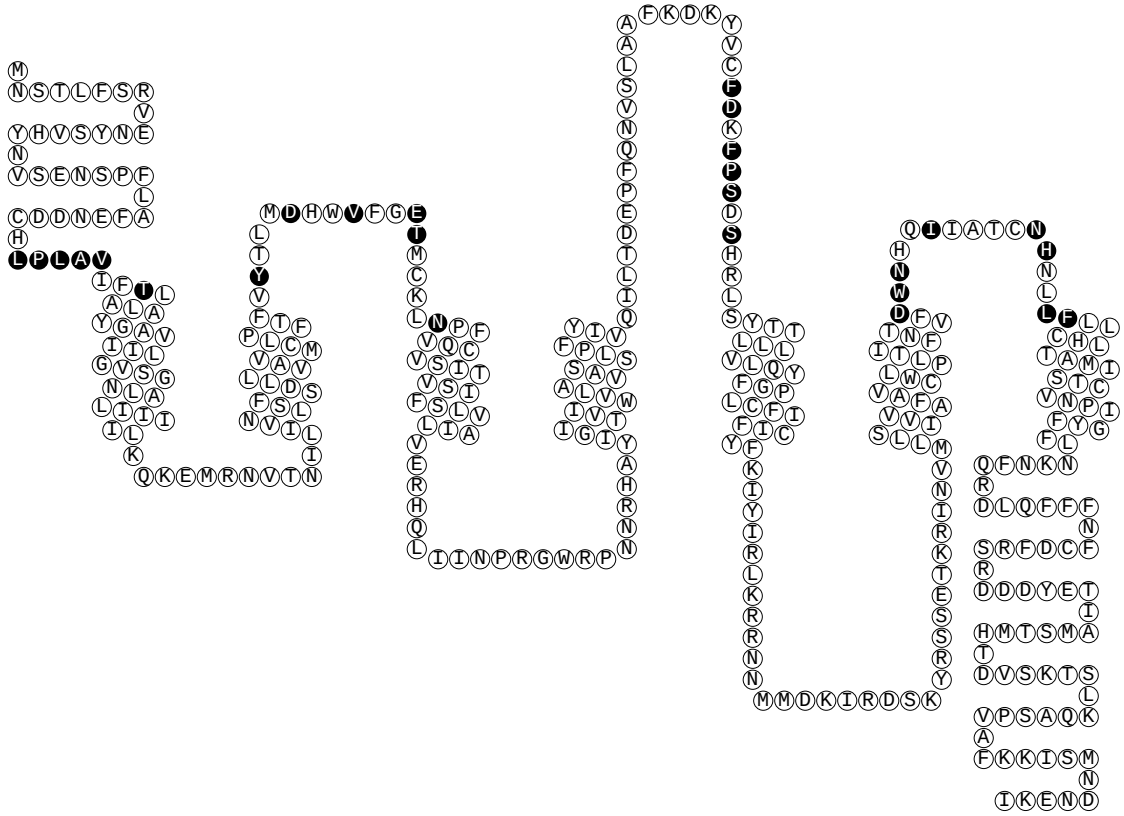

Scheme 1 *Localisations of TMHs in the amino acid sequence of the rY$_1$ receptor. Amino acid residues having van der Waals contacts with NPY in the energy minimized average of NPY - rY$_1$ structures between 140 and 180 ps of molecular dynaimcs simulation are indicated in bold. The scheme has been generated with the Viseur program (http://www.lctn.u-nancy.fr/viseur.html)*

was used to constrain bonds involving hydrogen atoms during the simulation. The step length was 0.001 ps, and the non-bonded pair list was updated after every 10 steps during the simulation.

Receptor modeling

The start and end positions of the TMHs are indicated in Scheme 1. Initial models of the TMHs were constructed from the rY$_1$ receptor sequence [14] with ϕ and Ψ angles at -57° and -47°, respectively. Each TMH was refined by energy minimization, and the water accessible surface and the electrostatic potentials 1.4 Å outside the surface were calculated with the MIDAS programs [27].

The GRAP database [24] was searched for point mutations affecting agonist binding to neuropeptide receptors at least 3-fold, compared to the wild type receptor, and to identify corresponding positions in the rY$_1$ sequence. Table 1 shows that the point mutations that affect agonist binding at least 3-fold are separated by 3-4 or 6-7 amino acids. Therefore, this observation indicates that these positions may be located at the same helical surface, line the central core of the receptor, and be directly involved in ligand binding or helical packing. The information obtained from the GRAP database was used as a guideline to pack the TMHs according to the projection map of visual rhodopsin [15] and to the proposed general arrangement of TMHs in GPCRs [16].The GRAP database did not contain site-directed mutagenesis results for amino acids in TMH1 of any neuropeptide receptor. TMH1 was orientated with Asn57, which is conserved in more that 80 % of all known GPCRs of family A, lining the central core of the model. The TMHs were packed such that the water accessible surface of the TMHs completely filled the gap between sequential TMHs, leaving an open central core containing the putative ligand binding site. Several different packing arrangements of the TMHs were considered, and the arrangement with the smoothest packing of the water accessible surfaces, and being most in agreement with the proposed arrangement of TMHs in GPCRs was used. The

closely packed 7-TMH bundle was refined by energy minimization.

Initial models of the loops and terminals were constructed based on secondary structure predictions by the Chou and Fasman method [28]. Amino acid residues predicted to have random coil conformation were used to bend the extracellular parts, so that residues important for binding of NPY to the rY_1 and hY_1 receptors, were positioned at the surface. Initial models of the N-terminal, C-terminal, intracellular and extracellular parts were energy minimized and then connected to the TMHs by interactive computer graphics. Site-directed mutagenesis studies of GPCRs have shown that a pair of cysteine residues in EC1 and EC2, that are conserved in most of the GPCRs, form a disulphide bond [22]. Therefore, a disulphide bond between Cys112 in EC1 and Cys197 in EC2 was introduced. The receptor model was energy-minimized, and further refined by 10 ps of molecular dynamics simulation. The TMHs and residues in the EC-parts identified from mutagenesis studies as important for binding of NPY (Leu35, Tyr99, Asp103, Asp199, Trp287, His297) [18-21], were kept at fixed positions during the energy minimization and molecular dynamics simulation using the belly option of the AMBER program. The final coordinate set from the molecular dynamics simulation was further refined by 20 ps of molecular dynamics simulation with all the loops and terminals free to move, while the TMHs were kept at fixed positions. The coordinates after 20 ps were energy minimized, and the water accessible surface [29] and potentials 1.4 Å outside the surface were calculated.

Modeling of NPY and docking into the rY_1 receptor

Although structures of human NPY in solution have been reported [2, 30] the initial model of NPY was constructed from the crystal structure of avian PP [1] by homology modeling. A similar approach has also been used by others to model NPY [18, 31, 32]. A monomer structure of NPY in solution [2] suggests that NPY has a three-dimensional structure similar to the crystal structure of avian PP, and to the structure of bovine PP in water [3], while a dimeric structure of NPY in solution suggests that the C-terminus of NPY dif-

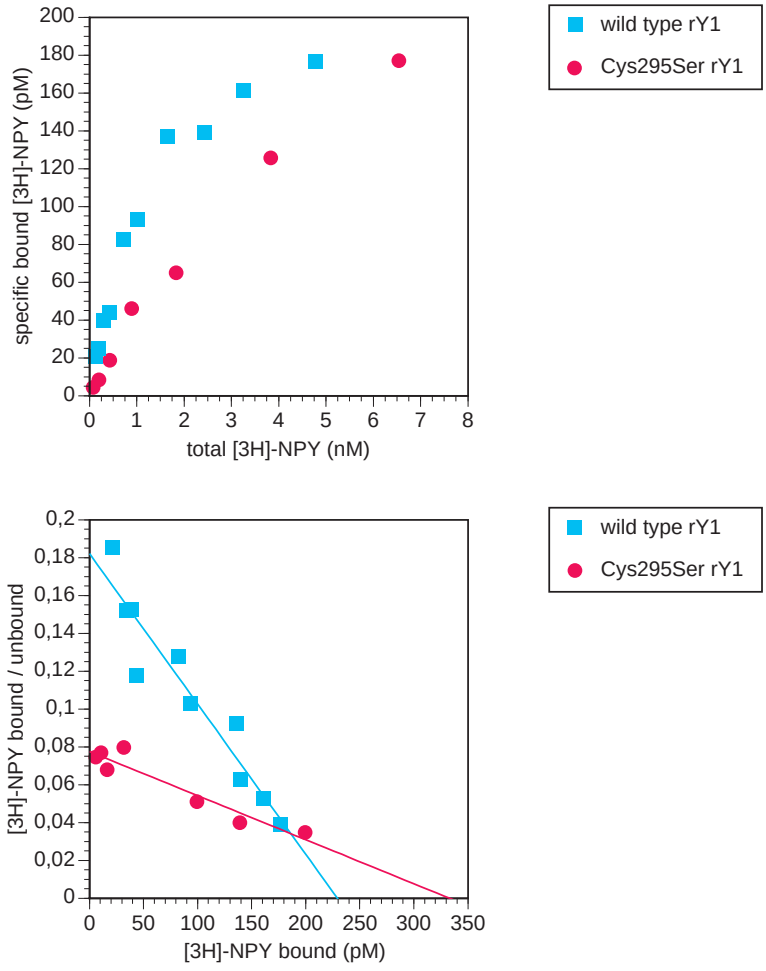

Figure 1 *Specific binding of ^{3}H-NPY to the wild type rY_1 receptor and the Cys295Ser rY_1 receptor mutant. The results shown are from a single experiment being representative for three separate experiments*

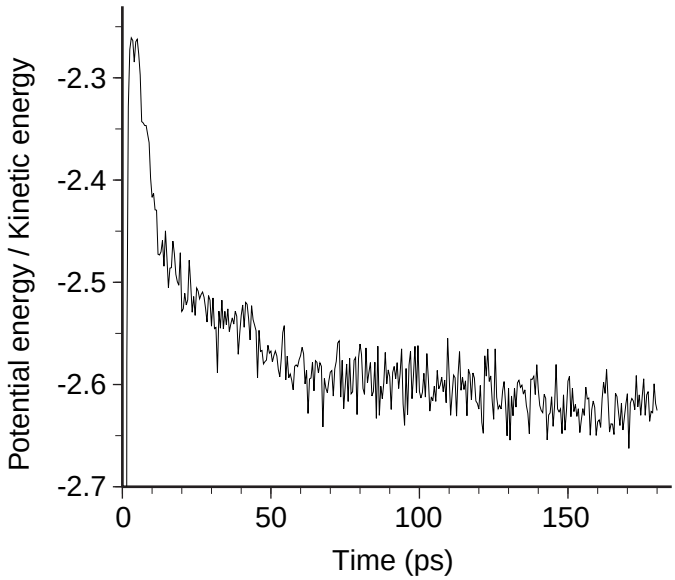

Figure 2 *Ratio between potential and kinetic energies of the NPY-rY$_1$ complex during 180 ps of molecular dynamics simulation*

fers from the crystal structure of avian PP and the structure of bovin PP in water [30]. The NPY model was energy minimized and used as start structure for a 110 ps molecular dynamics simulation of NPY. Different structures obtained during the simulation were energy minimized, and the water accessible surface and electrostatic potentials 1.4 Å outside the surface were calculated for the conformation with lowest energy.

Positions of negatively charged amino acids in the EC-parts of the receptor model and of positively charged amino acids in NPY, and water accessible surfaces and electrostatic potentials of NPY and the receptor, were used as guides in the docking of NPY into the receptor model. The best complementarity in the distribution of charged amino acids between the receptor and NPY was obtained when NPY was docked into the gap between EC1 and EC2 on one side, and the N-terminal and EC3 on the other side, with the C-terminal of NPY near the N-terminal of the receptor. Tyr1 in NPY was orientated towards Trp287 in EC3 and Asp286 at the EC-end of TMH6, whilst Lys4 in NPY was orientated in the direction of Asp199 in EC2. Arg33 in NPY was orientated towards Asp103 in EC1, and Arg35 in NPY towards Asp286 at the EC-end of TMH6. Tyr36 in NPY was located between Tyr99 in EC1 and His297 in EC3.

The NPY-receptor complex was refined by energy minimization and used as initial structure in a 180 ps molecular dynamics simulation of the NPY-rY$_1$ complex. The coordinates of the complex were saved every 1.0 ps during the simulation. The structurally flexible N-terminal of the rY$_1$ receptor contains sites (Asn2, Asn11 and Asn17) that most probably are glycosylated [21]. Since glycosylation of amino acids in the N-terminal not was included in the receptor model, a small harmonic potential was introduced, restraining the N-terminus (residue 1-38) in the Cartesian space during the simulation. The helices were not constrained during the simulation. An average structure was calculated from coordinate sets observed between 140 and 180 ps of simulation, and energy minimized. Molecular interaction energies between amino acids in NPY and in the receptor were calculated for the energy minimized average structure.

Docking of NPY$_{13-36}$ into the receptor model

A model of NPY$_{13-36}$ was constructed from the model of NPY and energy minimized until convergence. The NPY$_{13-36}$ model

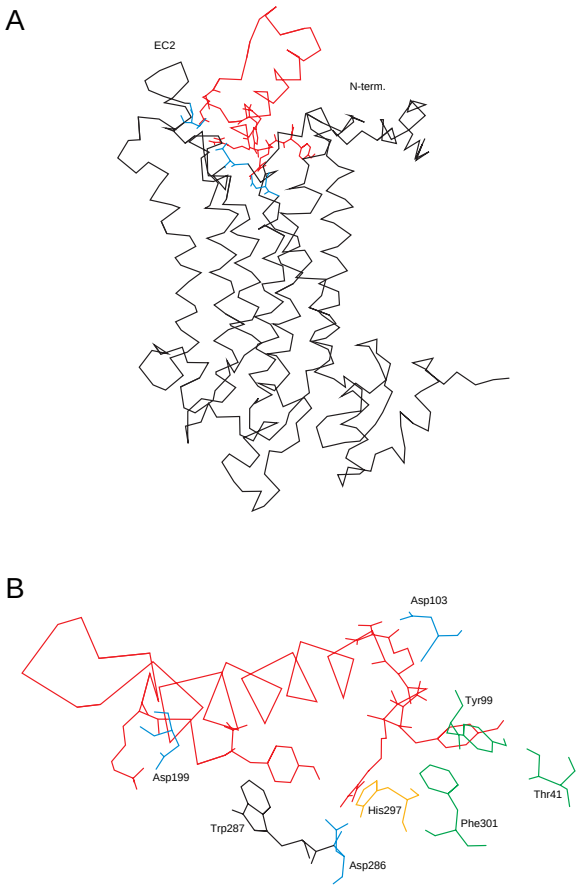

Figure 3 *Energy minimized average of NPY-rY$_1$ structures observed between 140 and 180 ps of molecular dynamics simulation. A: Viewed in the plane of the cell membrane (synaptic side up). Red: NPY, C_α atoms and side chains of* Tyr1, Lys4, Arg33, Arg35 *and* Tyr36, *black: C_α atoms of rY$_1$ receptor, blue: side chain of* Asp103, Asp199 *(EC2) and* Asp286. *B: Viewed from the extracellular side. Red: NPY, C_α atoms and side chains of* Tyr1 *(interacting with Asp286 and Trp287),* Lys4 *(interacting with Asp199),* Arg33 *(interacting with Asp103),* Arg35 *(interacting with Asp286 and His297),* Tyr36 *(interacting with Phe41, Tyr99 and Phe301)*

Table 2 *Binding affinities to rY_1 transiently expressed in COS-7 cells.*

K_d ^{3}H-NPY (nM)	1.8 ± 0.2	n=11
B_{max} ^{3}H-NPY (pmoles / mg protein)	0.9 ± 1.6	n=11
K_i NPY (nM)	1.2 ± 0.3	n=4
K_i [Leu31, Pro34]NPY (nM)	2.2 ± 0.6	n=4
K_i PYY (nM)	2.5 ± 0.5	n=3
K_i NPY_{13-36} (nM)	1100 ± 200	n=3

Table 3 *Binding affinity of ^{3}H-NPY to rY_1 mutants transiently expressed in COS-7 cells*

rY_1 5'nc receptor	**K_d (nM) (Mean value ± s.e.m.)**
Wild type	1.8 ± 0.2 (n=11)
Trp287Ser	no binding detected (n=3)
Trp287Gly	no binding detected (n=3)
Cys295Ser	5.1±1.1 (n=3)
His297Asn	no binding detected (n=3)

was docked into the receptor model using the energy minimized average rY_1-NPY complex as a template. The model of NPY_{13-36} was superimposed onto the NPY structure in the complex, NPY removed, and the NPY_{13-36}-rY_1 complex was energy minimized. The energy minimized complex was used as the initial structure in a 140 ps molecular dynamics simulation. The parameter protocol for the simulation was similar to that of the NPY-rY_1 receptor complex. An average structure was calculated from the coordinate sets between 100 and 140 ps, and energy minimized until convergence. Molecular interaction energies between amino acids in NPY_{13-36} and the receptor were calculated for the energy minimized average structure.

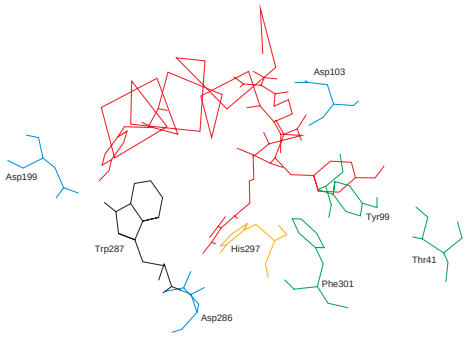

Figure 4 *Energy minimized average of NPY_{13-36} - rY_1 structures observed between 100 and 140 ps of molecular dynamics simulation, viewed from the extracellular side of the receptor. Red: NPY, C_α atoms and side chains of* Tyr27 *(interacting with Asp199 and Trp287),* Arg33 *(interacting with Asp103),* Arg35 *(interacting with Asp286 and His297),* Tyr36 *(interacting with Phe41, Tyr99 and Phe301)*

Results

Cloning of rY_1 cDNA

Combined PCR technology and screening of a cDNA library was used to clone a 1.53 kbp insert corresponding to the entire coding segment of the rY_1 receptor and a segment of 700 bp upstream of the initiating codon. The binding properties of the rY_1 receptor were tested after subcloning of the cDNA into the eucaryotic expression vector pcDNA3, and transient expression in COS-7 cells (Table 2). Scatchard analysis indicated the existence of a single binding site with a K_d value of 1.8 ± 0.2 nM. The rY_1 receptor bound PP peptide family members in the following rank order of relative potencies (Table 2): NPY > [Leu31, Pro34]NPY = PYY >> NPY_{13-36}. These relative potencies for the displacement of ^{3}H-NPY are in agreement with previously reported results [14].

Site-directed mutagenesis of the rY_1 receptor

The nucleotide sequences encoding Trp287, Cys295 or His297 were altered by site-directed mutagenesis, the mutated receptors were transiently expressed in COS-7 cells, and tested for thir ability to bind ^{3}H-NPY. The K_d values for the wild type and mutant receptors are summarized in Table 3. The Trp287Ser, Trp287Gly and His297Asn mutants all produced a receptor without detectable binding of NPY to the rY_1 receptor, while the Cys295Ser mutation decreased the affinity of NPY 2.8-fold, only. The specific binding of ^{3}H-NPY to the wild type rY_1 and the Cys295Ser mutant are shown in Figure 1.

The structure of the receptor model

The helical packing procedure resulted in a helical packing with TMH1 and TMH4 most exposed to the lipid membrane, while TMH3 was least exposed to the lipid membrane. The packing environments of amino acid residues used as guide-

Table 4 *Molecular interaction energies beteen amino acids in NPY and in the rY_1 receptor in the average energy minimized complex between 140 and 180 ps of simulation. All residues having van der Waals contact, and other residues (*) with interaction energy ≥ 2 kcal/mol or ≤ -2 kcal/mol, are included in the table*

NPY Residue	Receptor model Residue	Location	Energy (kcal/mol)	NPY Residue	Receptor model Residue	Location	Energy (kcal/mol)
Tyr1	Asn115	TMH3	-1.8	Leu30	Asn115	TMH3	-1.9
	Asp199*	EC2	-5.0	Arg33	Tyr99	EC1	-3.6
	Asp204*	EC2	-3.4		Asp103	EC1	-47.8
	Asp286*	TMH6	-4.8		Val106	EC1	-4.8
	Trp287	EC3	-4.3		Glu109	EC1	-29.8
	Asn288	EC3	-2.9		Thr100	EC1	-2.9
	His297	EC3	-1.5	Gln34	Tyr99*	EC1	-2.7
Pro2	Asp199	EC2	-3.9	Arg35	Tyr99*	EC1	-2.3
	Ser205	EC2	-9.8		Asp204*	EC2	-2.4
	Trp287	EC2	-1.8		Asp286	TMH6	-51.5
Ser3	Asp199	EC2	-5.3		Trp287	EC3	-1.5
Lys4	Asp199	EC2	-30.5		His297	EC3	-14.6
	Lys200*	EC2	3.6		Leu300	EC3	-0.8
	Phe201	EC2	-12.4	Tyr36	Asp31*	N-term.	-2.7
	Pro202	EC2	-5.2		Leu34	N-term.	-3.5
	Ser203	EC2	-13.9		Pro35	N-term.	-6.5
	Arg207	EC2	5.5		Leu36	N-term.	-6.4
Arg19	Ile291	EC3	-3.9		Ala37	N-term.	-5.5
	Ile292*	EC3	-2.4		Val38	N-term.	-2.3
Arg25	Asp31*	N-term.	-4.4		Thr41	N-term.	-0.2
	Leu34*	N-term.	-2.6		Tyr99	EC1	-6.9
His26	His297	EC3	-2.6		Asn296	EC3	-2.2
Tyr27	Phe198	EC2	-7.0		His297	EC3	-1.5
	Trp287	EC3	-0.5		Phe301	EC3	-3.3
Asn29	Pro35	N-term.	-2.8				

lines in the helical packing (Table 1) were: Asn57 in TMH1 was located between TMH2 and TMH7 forming a hydrogen bond with Asp85 in TMH2. Asp85 in TMH2 was also hydrogen bonded with Asn315 and Tyr319 in TMH7. The SH-group of Cys92 in TMH2 was located between the side chain of Ile50 in TMH1, and the side chains of Met309 and Thr312 in TMH7. The side chain of Thr96 in TMH2 was hydrogen bonded with the main chain carbonyl group of Tyr46 in TMH1. Asn115 in TMH3 interacted with the side chain of Asp286 in TMH6, while the side chain of Gln119 in TMH3 was facing between TMH5 and TMH6. The side chain of Cys120 in TMH3 was facing TMH4. The side chain of Phe172 in TMH4 formed a hydrogen bond with His206 in EC2, while the side chain of Phe175 in TMH4 was surrounded by the side chains of Leu114, Pro116, and Cys120 in TMH3 and the side chain of Leu214 in TMH5. The side chain of Thr211 in TMH5 was facing the side chain of Val284 in TMH6, while the side chain of Leu215 in TMH6 was directed towards Ile280 and Asn283 in TMH6. The side chain of Leu278 in TMH6 was located in a pocket consisting of the side chain of Cys274 in TMH6, Val314 and Phe318 in TMH7, while the side chain of Thr279 in TMH6 interacted with the side chain of Gln218 in TMH5 and Trp275 in TMH6. The side chain of Asn282 in TMH6 was involved in a hydrogen bond with Thr307 in TMH7. The side chain of Phe285 in TMH6 was packed against the side chain of Leu299 and Leu303 in TMH7, while the side chain of Asp286 in TMH6 interacted with the side chain of Asn115 in TMH3. The side chain of Cys304 in TMH7 interacted with the side chain Gln119 in TMH3 and the main chain carbonyl-group of Phe285 in TMH6, while the side chain of Met309 in TMH7 was located in a hydrophobic pocket consisting of the side chain of Tyr46 and Ile50 in TMH1 and Thr96 in TMH2. The side chain of Thr312 in TMH7 formed a hydrogen bond with the main chain carbonyl-group of His308 in TMH7 and interacted with Cys92 in TMH2, while the side chain of Asn315 in TMH7 was hydrogen bonded to the side chain of Asp85 in TMH2 and Tyr319 in TMH7.

The major part of the N-terminus was located distantly from the putative NPY binding site. However, the region outside His33-Val38 is facing into the central core of the receptor, capable of taking parts in binding to NPY. EC1 formed a relative flat span between TMH2 and TMH3 with the region Glu109-Leu114 packing against EC2. Asp103 which has been

Table 5 *Molecular interaction energies between amino acids in NPY_{13-36} and in the rY_1 receptor in the average, energy minimized complex between 100 and 140 ps of simulation. All residues having van der Waals contact, and other residues (*) with interaction energy ≥ 2.0 kcal/mol or ≤ -2 kcal/mol, are included in the table*

NPY_{13-36} Residue	Receptor model Residue	Location	Energy (kcal/mol)	NPY_{13-36} Residue	Receptor model Residue	Location	Energy (kcal/mol)
Glu15	Arg8*	N-term.	-3.0	Ile31	Phe191	EC2	-1.2
	Glu10*	N-term.	3.5		Cys197	EC2	-0.7
	Asp31*	N-term.	4.1	Arg33	Tyr99*	EC1	-2.6
	Cys32	N-term	-12.0		Asp103	EC1	-48.5
Asp16	Ile292	EC3	-2.6		Val106	EC1	-4.9
Arg19	Arg8*	N-term.	2.3		Glu109	EC1	-24.1
	Glu10*	N-term.	-2.5	Gln34	Tyr99	EC1	-9.0
	Asp31*	N-term.	-2.9		Met102	EC1	-2.0
	Leu34	N-term.	-1.1	Arg35	Glu109*	EC1	-2.2
	Ile292	EC3	-12.5		Asn115	TMH3	-8.6
Tyr20	Ile291	EC3	-2.5		Asp199*	EC2	-2.8
	Ile292	EC3	-3.5		Asp204*	EC2	-4.4
Ser22	Asn288	EC3	-5.1		Lys207*	EC2	6.0
Ala23	His289	EC3	-2.3		Asp286	TMH6	-32.8
Arg25	Asp31*	N-term.	-3.7		His297	EC3	-15.5
	Leu34	N-term.	-2.0		Phe301	TMH7	-2.5
His26	Trp287	EC3	-5.6	Tyr36	Pro35	N-term.	-8.0
	His297	EC3	-2.0		Ala37	N-term.	-2.4
Tyr27	Asp199	EC2	-14.7		Thr41	TMH1	-0.6
	Trp287	EC3	-2.5		Tyr99	EC1	-7.7
Leu30	Phe107	EC1	-1.1		Asn296	EC3	-2.9
	Trp287	EC3	-1.4		His297	EC3	-2.0
Ile31	Thr110	EC1	-2.8		Phe301	TMH7	-2.5

found to be important for binding of NPY [21] was located at the surface of the loop, with the side chain facing the central core created by the TMHs. EC2 was extending towards the EC-side of the receptor model with the Asp193, Lys192, Lys194 and Asp199 at the surface of the loop. The side chain of Glu181 in EC2 interacted strongly with the side chain of Lys113 in EC1 and with the side chain of Lys200 in EC2, which stabilized the structure of EC1 and EC2. Ser187 interacted with Glu109 and Thr110 in EC1. EC3 formed a rather short span between TMH6 and TMH7 with Trp287 and His297 at the surface of the loop with their side chains facing into the central core of the receptor, capable of forming ligand binding interactions. The region outside Ala293-Asn296 in EC3 was packed against the region outside His33-Pro36 in the N-terminus.

Peptide-rY_1 interactions

The aim of the molecular dynamics simulation of NPY and NPY_{13-36} with the rY1 receptor was to minimize the energy of the molecular complex and avoid unfavourable non-bonded interactions, and not to study time dependent structural changes. The potential/kinetic energy curve shown in Figure 2 indicates that an energetically stable complex between NPY and the receptor model was obtained during the simulation.

In the calculation of the interaction energies, factors like changes in conformation and entropy upon binding are not taken into account. Therefore, the interaction energies in Table 4 and 5 are not directly correlated to experimental ligand binding affinities. Amino acid residues in Table 4 and 5 must be considered as important residues for stabilizing the peptide-rY_1 complex.

In the energy minimized NPY-rY_1 complex that was used as start structure for the simulation, the longitudinal axis of NPY was tilted about 20° relative to the helical axes of the TMHs. Tyr1 of NPY was hydrogen-bonded with Asp286 at the EC-end of TMH6, had aromatic interactions with Trp287 in EC3, and had electrostatic interactions with Asp199 and Asp204 in EC2. Lys4 in NPY had strong electrostatic interactions with Asp199 in EC2, while Arg33 in NPY formed a salt bridge with Asp103 in EC1 of the receptor. Arg35 in NPY had electrostatic interactions with Asp286 at the EC-end of TMH6, was hydrogen bonded with His297 in EC3, and had electrostatic interactions with Leu34 in the N-terminal of the receptor. The hydroxyl group of the amidated Tyr36

in NPY was hydrogen bonded with Tyr99 in EC1 and interacted with His297 in EC3.

In the energy refined, average coordinate set from the NPY-rY_1 structures observed between 140 and 180 ps of simulation, the longitudinal NPY axis had become tilted about 45° relative to the helical axes of the TMHs. More amino acids in the receptor model were involved in NPY interactions in the complex after 140-180 ps of simulation than before the simulation. The interactions of Tyr1 in NPY with Asp286 and Trp287 were maintained during the simulation, and a hydrogen bond was formed between Tyr1 and Asn115 at the EC-end of TMH3. Tyr1 also interacted with His297 in EC3. Lys4 of NPY still interacted with Asp199 in EC2, while Arg25 of NPY interacted with Leu34 in the N-terminal of the receptor. Tyr27 of NPY was in a pocket between Phe198 in EC2 and Trp287 in EC3. Arg35 in NPY formed a salt bridge with Asp286 at the EC-end of TMH6, and was hydrogen bonded with His297. The hydroxyl group of Tyr36 in NPY was hydrogen bonded with the side chain of Thr41 in the N-terminal of the receptor, and with Tyr99 in EC1. Tyr36 in NPY also interacted with Asn296 and His297 in EC3, and had aromatic interactions with Phe301 in EC3 (Figure 3).

During the simulation of the NPY-rY_1 complex, conformational changes occurred in the N- and C-terminal parts of NPY. These changes were largest in the N-terminal region, where a kink was introduced at Pro5. Compared to the initial structure, the N-C_α-C_β-C_γ torsional angles of Arg33, Arg35 and Tyr36 of NPY had changed by 95°, 90° and 60°, respectively, in the average structure from 140-180 ps of simulation.

The energy refined, average coordinate set from the NPY_{13-36}-rY_1 structures observed between 100 and 140 ps of simulation indicated that NPY_{13-36} interacted weaker with amino acids in EC2 of the receptor than did NPY (Table 4 and 5). Tyr1 and Lys4 in NPY interacted strongly with the region outside Asp199-Asp204, and contributed strongly to the stabilization of the complex, while only Tyr27 in NPY_{13-36} interacted strongly with this region of the receptor. The peptide - receptor model complexes suggested that the binding modes of Arg33, Arg35 and Tyr36 of NPY_{13-36} at the receptor were similar to the corresponding amino acids in NPY (Figure 4 and 5). However, the interactions of Arg35 with Asp286 in the receptor were much stronger in the NPY-rY_1 receptor complex than in the NPY_{13-36}-rY_1 receptor complex (Table 4 and 5).

Discussion

The molecular dynamics refinements of loops and terminals in the model building were performed to avoid unfavourable non-bonded interactions. The overall architecture of the loops did not change much during the refinements. Altogether, the total MD relaxation time on loops and terminals was 30 ps. Further, the flexibility allowed during molecular dynamics simulations of receptor-ligand interactions would also diminish the effect of the relatively crude secondary structure prediction of the loops and terminals.

A fixed dielectricity constant (ε =4) is usually used to simulate the effects of lipid membranes, and has previously been used in molecular dynamics simulation of ligand - receptor interactions when loops and terminals are not included in the complex [33, 34]. However, when the complex included loop and terminal sequences, and water molecules were not included, a distance-dependent dielectric function was used for the entire model [35-37] to simulate the effects of EC and IC water molecules. Therefore, without having the possibility of treating the loops differently from the transmembrane side chains, and without explicit water molecules in the system, a distance dependent dielectric function was used in the present study.

Molecules that exert their effects by binding to GPCRs are extremely diverse, ranging from small molecules like catecholamines to peptides like NPY, and glycoprotein hormones. The agonist binding sites of catecholaminergic receptors are well characterized, and have been found to include mainly amino acids in the TMHs of the receptors. Much less is known about the agonist binding sites of peptides and proteins to GPCRs. However, the interactions of peptides and proteins with GPCRs seem to involve amino acids in both the TMHs and EC-parts of the receptor [18-20, 38-40]. In a previous study we have identified amino acids in the N-terminal, EC1, EC2 and TMH6 of the rY_1 receptor which are important for binding of NPY [21]. The present study suggests that amino acids in EC3 are also important for binding of NPY.

In the energy minimized NPY-receptor complex after 140-180 ps of simulation, Trp287 in EC3 had aromatic interactions with both Tyr1 and Tyr27 of NPY, and also interacted with Arg35 in the C-terminal of NPY. Trp287 contributed to the stabilization of the three-dimensional receptor structure via aromatic interactions with Tyr210 of TMH6 and interactions with Asn115 in TMH3. The interactions of Trp287 with NPY and with residues in TMH3 and TMH6, and the loss of affinity for the Trp287Ser and Trp287Gly mutants (Table 3), suggest that a bulky aromatic side chain at the position of Trp287 is required, both for maintaining a correct receptor structure and for a proper interaction with NPY. Mutation of the corresponding tryptophane residue in the hY_1 receptor, which also resulted in loss of affinity for NPY, did not impair the membrane expression of the receptor [20]. However, impaired membrane expression of the Trp287Ser and Trp287Gly mutants can not be completely ruled out.

Mutation of His297 to an alanine abolished the binding of NPY (Table 3). The corresponding mutation of the hY_1 receptor, which also resulted in loss of affinity for NPY, did not to impair the membrane expression of the receptor [19, 20]. In the average, energy minimized complex between 140 and 180 ps of simulation, His297 in EC3 was hydrogen bonded with Arg35 in NPY, and had interactions with the aromatic residues Tyr1 and Tyr36 of NPY (Figure 3). An asparagine side chain at a position corresponding to that of His297 would be unable to form a hydrogen bond with Arg35, and would

also prevent the interactions with Tyr1 and Tyr36, which may explain the loss of affinity for the His297Asn mutant.

During the simulation Leu34 in rY_1 interacted with Arg25 and Tyr36 in NPY (Table 4). This is in agreement with our previous study which demonstrated that substitution of Leu34 in rY_1 by arginine decreased the affinity for ^{3}H-NPY 2.7 - fold, while substitution of Leu34 with glutamic acid slightly increased the affinity for ^{3}H-NPY [21]. Relatively weak Y_1 receptor interactions of Arg25 in NPY was also shown in an other study which demonstrated that substitution of Arg25 in NPY with lysine only slightly reduced Y_1 receptor binding affinity, while substitution of Arg33 and Arg35 resulted in a more pronounced decrease in Y_1 affinity [41]. Therefore, in spite of that the potential energies in Table 4 are not directly connected to receptor binding affinities, it is interesting to note, that Arg33 and Arg35 in NPY had strong receptor interactions after complexation (Table 4).

Studies of substituted and truncated analogs of NPY have shown that the Y_1 receptor needs an intact N-terminal of NPY to become fully activated [42], and it has been proposed that Tyr1 in NPY is important for Y_1 receptor recognition [43]. In the average complex between 140 and 180 ps of simulation, Tyr1 had electrostatic interactions with Asp286, was hydrogen bonded with Asn115 at the EC-end of TMH3, had aromatic interactions with Trp287 and interacted with His297 in EC3. The relatively strong interaction energy between Tyr1 and the receptor model indicates that this residue may contributes to NPY-rY_1 interactions and not only to the initial receptor recognition.

Receptor binding studies have shown that the N-terminal truncated NPY-analog NPY_{13-36} has much lower affinity for the rY_1 receptor than NPY [4, 5]. Figure 3 and 4 indicate that the main differences in rY_1 receptor binding mode between NPY_{13-36} and NPY are the interactions with amino acid residues in EC2. Tyr1 and Lys4 in NPY interacted strongly with the region outside Asp199-Asp204 in the receptor model, while NPY_{13-36} interacted only weakly with this region of the receptor (Table 5). This observation may indicates that the interactions of Tyr1 and Lys4 with EC2 are important for the affinity of NPY to the rY_1 receptor. EC2 is connected to IC3 via TMH5, and IC3 has been shown to be very important for coupling to G-proteins in GPCRs [44, 45]. Therefore, lack of interactions with amino acid residues in EC2 may explain way N-terminal truncated analogs of NPY not fully activate the rY_1 receptor [42].

The amidated Tyr36 at the C-terminal of NPY is important for Y_1 receptor binding [19, 46, 47]. Site-directed mutagenesis studies of the hY_1 receptor have suggested that Tyr36 of NPY interacts with the Y_1 receptor via at least two hydrogen bonds, possibly between the hydroxyl group of Tyr36 and a tyrosine corresponding to Tyr99 in the rY_1 receptor, and between the amide group of Tyr36 and a histidine corresponding to His297 in the rY_1 receptor [19]. In the energy minimized complex from 140-180 ps of simulation, two hydrogen bonds were formed by the hydroxyl group of Tyr36 in NPY, one with Thr41 in the N-terminal of the receptor and one with Tyr99 in EC1. The amide group of Tyr36 did not take part in interactions with the receptor (Figure 3). These interactions were also maintained during the simulation of NPY_{13-36} - rY_1 receptor interactions (Figure 4) This is in agreement with conformational studies of isolated PP fragments which have indicated that the main function of the amide group of Tyr36 is to maintain an appropriate structure of NPY for interaction with the Y_1 receptor, and not to directly take part in Y_1 receptor interactions [48].

Site-directed mutagenesis experiments have shown that a pair of cysteine residues in EC1 and EC2, which are conserved in many GPCRs, form a disulphide bond [22]. The rY_1 and several other GPRCs also have cysteine residues in the N-terminal and in EC3, and this pair of cysteines form a disulphide bond in the angiotensin II AT_{1a} receptor [23]. However, the Cys295Ser mutant only had slightly decreased affinity for ^{3}H-NPY compared to the wild type receptor (Table 3). For family A receptors, site-directed mutagenesis studies of cysteine residues corresponding to Cys112 in EC1 or Cys197 in EC2 of the rY_1 receptor have resulted in very a low binding or no binding at all [24], such that a 2.8 fold decrease in ^{3}H-NPY binding compared with the wild type receptor seem not to be significant with Cys295 being involved in a disulphide bond, and a disulphide bond was therefore not included between Cys32 and Cys295 in the rY_1 model.

Site-directed mutagenesis studies of the hY_1 receptor have shown that alanine substitution of residues corresponding to Trp162, Phe172, Gln218 or Asn282 in the rY_1 receptor, all induced a nearly complete loss of affinity for NPY [20]. The present rY_1 model suggests that the lack of NPY affinity for these mutants may be due to overall conformational changes of the receptor. The model places Trp162 and Gln218 three helical turns from the extracellular ends of the TMHs, in positions not directly involved in NPY binding. However, both Trp162 and Gln218 stabilized helical packing via interactions with other TMHs, Trp162 with residues in TMH3 and Gln218 with Ser126 in TMH3 and Thr279 in TMH6. Asn282 was located two helical turns from the extracellular end of TMH6. During the simulation, Asn282 was hydrogen bonded with Thr307 in TMH7, and had only weak interactions (~ -0.5 kcal/mol) with Arg35 of NPY. Phe172, which was near the extracellular end of TMH4, interacted with Pro116, Phe117 and Cys120 in TMH3 and with Leu214 in TMH5 during the simulation. An alanine or an other residue with a small side chain at positions corresponding to those of Trp162, Phe172, Gln218 or Asn282, might obliterate such interactions and thus interfere with the three-dimensional receptor structure.

A previous molecular modeling study of the hY_1 receptor [32] suggests that amino acid residues in the C-terminus of NPY interacts with amino acids in TMH3, TMH5, TMH6 and TMH7. This position of the C-terminus of NPY relative to the receptor model is very similar to the position of the C-terminus in the present study. However, the study by Du et al. [32] positioned NPY deeper in the helical core than in the present study, and proposed direct interactions between NPY and Gln218 (Gln219 in the hY_1 receptor). In the present model, a direct interaction with Gln218 seems unlikely since Gln218 is located three helical turns from the extracellular

end of the TMHs, interacting with Ser126 in TMH3 and Thr279 in TMH6.

Site-directed mutagenesis and molecular modeling studies of the gonadotropin-releasing hormone receptor [49] and the 5-HT_{2a} receptor [50] have suggested that an aspartic acid in TMH2 is hydrogen-bonded with an asparagine in TMH7. These amino acids, which are highly conserved among GPRCs, correspond to Asp85 and Asn315 in the rY_1 receptor. Asp85 and Asn315 formed a hydrogen bond which was maintained during the simulation of the NPY-rY_1 complex. The simulation introduced conformational changes in the TMHs which involved Asp85 and Asn315 in a hydrogen bonding network with Asn57 in TMH1 and Tyr319 in TMH7.

NPY and other members of the PP-family have a large dipole moment antiparallel to the dipole created by the α-helical structure, which produces a highly positive area outside the putative receptor binding region in the N- and C-terminal ends of NPY [31]. The charge distribution of NPY suggests that its binding to the rY_1 receptor is initiated by electrostatic interactions with negatively charged amino acids in the extracellular domains of the Y_1 receptor. The present simulation of NPY-rY_1 interactions suggests that NPY binds to amino acids located in the extracellular domains of the receptor and near the extracellular ends of some of the TMHs. Binding of NPY may thereby induce conformational changes in the TMHs creating the observed hydrogen bonding network consisting of Asn57, Asp85, Asn315 and Tyr319, leading to a specific receptor conformation required for signal transduction.

These molecular modeling and site-directed mutagenesis studies have demonstrated the value of using computational methods together with experimental techniques to characterize the ligand binding site of GPCRs. However, while the projection map of visual rhodopsin enables construction of quite reliable models of the TMHs of GPCRs, the structures of the extra- and intracellular parts remain more uncertain. In spite of this, the available results from site-directed mutagenesis studies with the human and rat Y_1 receptors have, in our view, enabled the construction of a fairly reliable model of NPY-Y_1 receptor interactions, which is supported by available structure - activity relationships data for NPY. The results suggest that the N-terminal Tyr1 in NPY binds to a pocket formed by Asp286, Trp287, His297 and Asn115, that Lys4 and Arg33 in NPY interact strongly with Asp199 and Asp103, respectively, and that Arg35 in NPY interacts with both Asp286 and His297. The present model also suggests that the side chain of Tyr36 in receptor bound NPY is located in a pocket formed by Thr41, Tyr99, Asn296, His297 and Phe301.

References

1. Blundell, T.L.; Pitts, J.E.; Tickle, I.J.; Wood, S.P. and Wu, C.-W. *Proc. Natl. Acad. Sci. USA* **1981**, *78* 4175.
2. Darbon, H.; Bernassau, J.M.; Deleuze, C.; Chenu, J.; Roussel, A. and Camillau, C. *Eur. J. Biochem.* **1992**, *209*, 765.
3. Li, X.A.; Sutcliffe, M.J.; Schwartz, T.W. and Dobson, C.M. *Biochemistry* **1992**, *31*, 1245.
4. Herzog, H.; Hort, Y.J.; Ball, H.J.; Hayes, G.; Shine, J. and Selbie, L.A. *Proc. Natl. Acad. Sci. USA.* **1992**, *89*, 5794.
5. Larhammar, D.; Blomqvist, A.G.; Yee, F.; Jazin, E.; Yoo, H. and Wahlested, C. *J. Biol. Chem.* **1992**, *267*, 10935.
6. Rose, P.M.; Fernandes, P.; Lynch, J.S.; Frazier, S.T.; Fisher, S.M.; Kodukula, K.; Kienzle, B. and Seethala, R. *J. Biol. Chem.* **1995**, *270*, 22661.
7. Wahlestedt, C.; Regunathan, S. and Reis, D.J. *Life Science* **1992**, *50*, 8.
8. Bard, J.A.; Walker, M.W.; Branchek, T.A. and Weinshank, R.L. *J. Biol. Chem.* **1995**, *270*, 26762.
9. Lundell, I.; Blomqvist, A.G.; Berglund, M.M.; Schober, D.A.; Johnson, D.; Statnick, M.A.; Gadski, R.A.; Gehlert, D.R. and Larhammar, D. *J. Biol. Chem*. **1995**, *270*, 29123.
10. Gerald, C.; Walker, M.W.; Criscione, L.; Gustafson, E.L.; Batzl-Hartmann, C.; Smith, K.E.; Vaysse, P.; Durkin, M.M.; Laz, T.M.; Linemeyer, D.L.; Schaffhauser, A.O.; Whitebread, S.; Hofbauer, K.G.; Taber, R.I; Branchek, T.A.; and Weinshank, R. *Nature* **1996**, *382*, 168.
11. Weinberg, D.H.; Sirinathsinghji, D.J.S.; Tan, C.P.; Shiao, L.-L.; Morin, N.; Rigby, M.R.; Heavens, R.H.; Rapoport, D.R.; Bayne, M.L.; Cascieri, M.A.; Strader, C.D.; Linemeyer, D.L. and MacNeil, D. *J. Biol. Chem.* **1996**, *271*, 16435.
12. Cox, H.M. and Tough, I.R. *Br. J. Pharmacol.* **1995**, *116*, 2673.
13. Eva, C.; Keinanen, K.; Monyer, H.; Seeburg, P. and Sprengel, R. *FEBS. Lett.* **1990**, *271*, 81.
14. Krause, J.; Eva, C.; Seeburg, P.H. and Sprengel, R. *Mol. Pharmacol.* **1992**, *41*, 817.
15. Schertler, G.F.X.; Villa, C. and Henderson, R. *Nature* **1993**, *362*, 770.
16. Baldwin, J.M. *EMBO J.* **1993**, *12*, 1693.
17. Unger, V.M.; Hargrave, P.A.; Baldwin, J.M. and Schertler, G.F.X. *Nature* **1997**, *389*, 203.
18. Walker, P.; Munoz, M.; Martinez, R. and Peitsch, M. *J. Biol. Chem.* **1994**, *269*, 2863.
19. Sautel, M.; Martinez, R.; Munoz, M.; Peitsch, M.C.; Beck-Sickinger, A.G. and Walker, P. *Mol. Cell Endocrinol.* **1995**, *112*, 215.
20. Sautel, M.; Rudolf, K.; Wittneben, H.; Herzog, H.; Martinez, R.; Munoz, M.; Eberlein, W.; Engel, W.; Walker, P. and Beck-Sickinger, A.G. *Mol. Pharmacol.* **1996**, *50*, 285.
21. Robin-Jagerschmidt, C.; Sylte, I.; Bihoreau, C.; Hendricksen, L.; Calvet, A.; Dahl, S.G. and Bénicourt, C. *Mol. Cell. Endocrinol.* **1998**, in press.
22. Savarese, T.M. and Fraser, C.M. *Biochem. J.*, **1992**, *283*, 1.
23. Yamano, Y.; Ohyama, K.; Chaki, S.; Guo, D.F. and Inagami, T. Biochem. Biophys. Res. Commun. **1992**, *187*, 1426.
24. Kristiansen, K; Dahl, S.G. and Edvardsen, Ø. *Proteins: Struct. Funct. Genetics* **1996**, *26*, 81.

25. McPherson, G.A. *Comput. Programs. Biomed*. **1983**, *17*, 107.
26. Weiner, S.J.; Kollman, P.A.; Case, D.A.; Singh, U.C.; Ghio, C.; Alagona, G.; Profeta Jr., S. and Weiner, P. *J. Am. Chem. Soc.* **1984**, *106,* 765.
27. Ferrin, T.E.; Huang, C.C.; Jarvis, L.E. and Langridge, R. *J. Mol. Graph.* **1988**, *6*, 1.
28. Chou, P.Y. and Fasman, G.D. *Annu. Rev. Biochem.* **1978**, *47*, 251.
29. Connolly, M.L. *Science*, **1983**, *221*, 709.
30. Cowley, D.J.; Hoflack, J.M.; Pleton, J.T. and Saudek, V. *Eur. J. Biochem*. **1992**, *205*, 1099.
31. Bjørnholm, B.; Jørgensen, F.S. and Schwartz, T.W. *Biochemistry* **1993**, *32*, 2954.
32. Du, P.; Salon, J.A.; Tamm, J.A.; Hou, C.; Cui, W.; Walker, M.W.; Adham, N.; Dhanoa, D.S.; Islam, I.; Vaysse, P.J-J.; Dowling, B.; Shifman, Y.; Boyle, N.; Rueger, H.; Schmidlin, T.; Yamaguchi, Y.; Branchek, T.A.; Weinshank, R.L. and Gluchowski, C.G. *Prot. Engn*. **1997**, *10*, 109.
33. Zhang, D. and Weinstein, H. *J. Med. Chem.* **1993,** *36*, 934.
34. Luo, X.; Zhang, D. and Weinstein, H. *Protein Engn.* **1994,** *7*, 1441.
35. Fanelli, F.; Menziani, M.C. and De Bendetti, P.G. *Biorg. Med. Chem.* **1995,** *3*, 1465.
36. Sheer, A.; Fanelli, F.; Costa, T.; De Benedetti, P.G. and Cotecchia, S. *EMBO J.* **1996,** *15*, 3566.
37. Sylte, I.; Edvardsen, Ø. and Dahl, S.G. *Protein Engn.* **1996,** *9*, 149.
38. Fong, T.M.; Huang, R.R. and Strader, C.D. *J. Biol. Chem*. **1992**, *267*, 25664.
39. Hjorth, S.A.; Schambye, H.T.; Greenlee, W.J. and Schwartz, T.W. *J. Biol. Chem*. **1994**, *269*, 30953.
40. Novotny, E.A.; Bednar, D.L.; Connolly, M.A.; Connor, J.R. and Stormann, T.M. *Biochem. Biophys. Res. Commun.*, **1994**, *201*, 523.
41. Fournier, A.; Gagnon, D.; Quirion, R.; Dumont, Y.; Pheng, L-H. and St-Pierre, S. *Mol. Pharmacol.* **1994**, *45*, 93.
42. Grundemar, L.; Krstenansky, J.L. and Håkanson, R. *Eur. J. Pharmcol.* **1993**, *323*, 271.
43. Martel, J.C.; Fournier, A.; St Pierre, S.; Dumont, Y.; Forest, M. and Quirion, R. *Mol. Pharmacol.* **1990**, *38*, 494.
44. Liu, J.; Blin, N.; Conklin, B.R. and Wess, L. *J. Biol. Chem.* **1996**, *271*, 6172.
45. Damaj, B.B.; McColl, S.R.; Neote, K.; Songqing, N.; Ogborn, K.T.; Hebert, C.A. and Naccache, P.H. *FASEB J.* **1996**, *10*, 1426.
46. Kirby, D.A.; Boublik, J.H. and Rivier, J.E. *J. Med. Chem.* **1993**, *36*, 3802.
47. Kirby, D.A.; Koerber, S.C.; Craig, A.G.; Feinstein, R.D.; Delmas, L.; Brown, M.R. and Rivier, J.E. *J. Med. Chem.* **1993**, *36*, 385.
48. Tonan, K.; Kawata, Y. and Hamaguchi, K. *Biochemistry*, **1990**, *29*, 4424.
49. Zhou, W.; Flanagan, C.; Ballesteros, J.A.; Konvicka, K.; Davidson, J.S.; Weinstein, H.; Millar, R.P. and Sealfon, S.C. *Mol. Pharmacol.* **1994**, *45*, 165.
50. Sealfon, S.C.; Chi, L.; Ebersole, B.J.; Rodie, V.; Zhang, D.; Ballesteros, J.A. and Weinstein, H. *J. Biol. Chem*. **1995**, *270*, 16683.
51. Bihoreau, C.; Monnot, C.; Davies, E.; Teutsch, B.; Bernstein, K.E.; Corvol, P. and Clauser, E. *Proc. Natl. Acad. Sci. USA* **1993**, *90*, 5133.
52. Kong, H.; Raynor, K.; Yasuda, K.; Moe, S.T.; Portoghese, P.S.; Bell, G.I. and Reisine, T. *J. Biol. Chem*. **1993**, *268*, 23055.
53. Surratt, C.K.; Johnson, P.S.; Moriwaki, A.; Seidleck, B.K.; Blaschak, C.J.; Wang, J.B. and Uhl, G.R. *J. Biol. Chem*. **1994**, *269*, 20548.
54. Perlman, J.H.; Nussenzveig, D.R.; Osman, R. and Gershengom, M.C. *J. Biol. Chem.* **1992**, *267*, 24413.
55. Flanagan, C.A.; Becker, I.I.; Davidson, J.S.; Wakefield, I.K.; Zhou, W.; Sealfon, S.C. and Millar, R.P. *J. Biol. Chem*. **1994**, *269*, 22636.
56. Huang, R.R.; Yu, H.; Strader, C.D. and Fong, T.M. *Biochemistry* **1994**, *33*, 3007.
57. Rosenkilde, M.M.; Cahir, M.; Gether, U.; Hjort, S.A. and Schwartz, T.W. *J. Biol. Chem.*, **1994**, *269*, 28160.
58. Bhogal, N.; Donnelly, D. and Findlay, J.B.C. *J. Biol. Chem.* **1994**, *269*, 27269.
59. Zhu, G.; Wu, L.H.; Mauzy, C.; Egloff, A.M.; Mirzadegan, T. and Chung, F.Z. *J. Cell Biochem.*, **1992**, *50*, 159.
60. Perlman, J.H.; Thaw, C.N.; Laakkonen, C.Y.; Bowers, C.Y.; Osman, R. and Gershengom, M.C. *J. Biol. Chem.*, **1994**, *269*, 1610.
61. Freedman, R. and Jarnagin, K. *Agents. Actions. Suppl.* **1992**, *38*, 487.
62. Frändberg, P.-A.; Muceniece, R.; Prusis, P.; Wikberg, J. and Chhajlani, V. *Biochem Biophys. Res. Commun.* **1994**, *202*, 1266.
63. Nardone, J. and Hogan, P.G. *Proc. Natl. Acad. Sci. USA* **1994**, *91*, 4417.
64. Gether, U.; Nilsson, L.; Lowe III, J.A. and Schwartz, T.W. *J. Biol. Chem.* **1994**, *269*. 23959.
65. Marie, J.; Maigret, B.; Joseph, M.P.; Larguier, R.; Nouet, S.; Lombard, C. and Bonnafous, J.C. *J.Biol. Chem.* **1994**, *269*, 20815.
66. Schambye, H.T.; Hjorth, S.A.; Bergsma, D.J.; Sathe, G. and Schwartz, T.W. *Proc. Natl. Acad. Sci. USA* **1994**, *91*, 7046.